Re-evaluations of seismic hazard of Iraq

AbdulMuttalib Isa Said & Mustafa Shakir Farman

Arabian Journal of Geosciences

ISSN 1866-7511
Volume 11
Number 11

Arab J Geosci (2018) 11:1-19
DOI 10.1007/s12517-018-3558-7

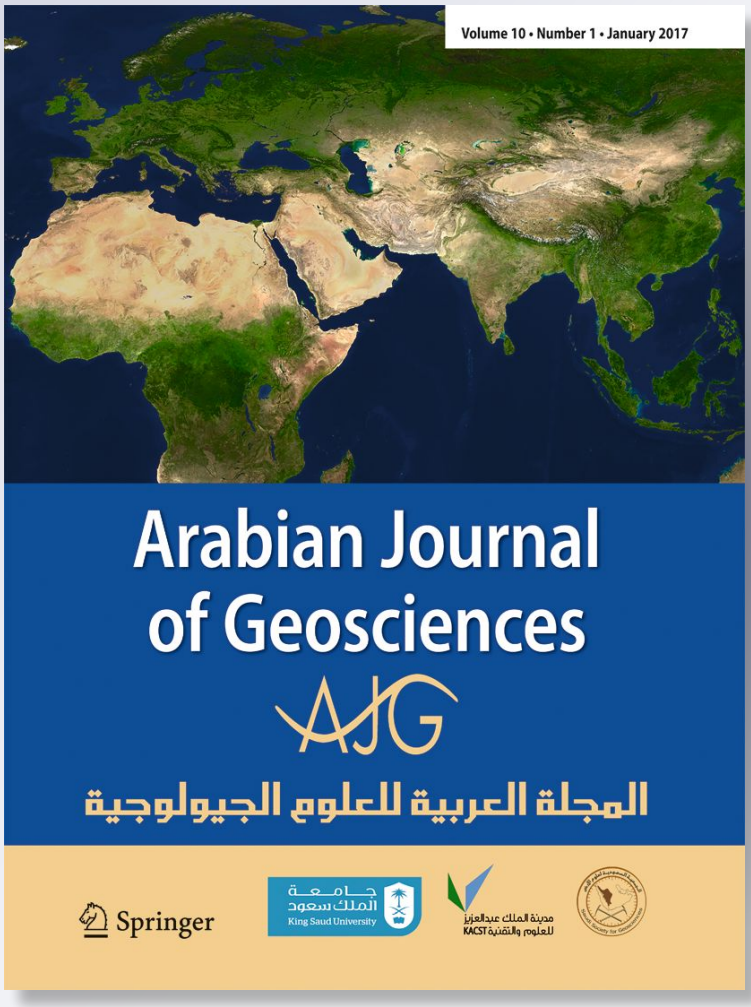

Springer

Arabian Journal of Geosciences (2018) 11:279
https://doi.org/10.1007/s12517-018-3558-7

ORIGINAL PAPER

Re-evaluations of seismic hazard of Iraq

AbdulMuttalib Isa Said[1] · Mustafa Shakir Farman[2]

Received: 19 April 2017 / Accepted: 18 April 2018

Abstract

In recent years, Iraq has experienced an increase in seismic activity, especially, near the east boundary with Iran. Previous studies present their results in terms of PGA and for return periods of 500 years and less, and other studies not continued to include the whole PSHA process whereas some recent studies continued to include the whole PSHA process using earthquakes data till 2009 including dependent events. This study includes two main stages, the first is collecting the earthquakes records including the recent events till the end of March 2016 and applying data processing to get the net catalog to independent events. The second stage is applying the steps of PSHA method. Matlab programs have been built to execute these two stages and to convert the results of PSHA computations into contours of 5% damping PGA and spectral accelerations at 0.2 and 1.0 s for a return period of 2475 years, and for rock sites. Also, spectral acceleration against period has been presented for main cities. Also, the PGA map, for a return period of 475 years, has been plotted and then prepared together with similar maps of neighbor countries in one map for comparison. In general, this comparison indicates the similarity in behavior but, the values reveal a relative agreement and they are between Turkish and Iranian values.

Keywords Iraq · PSHA · Data processing · Independent events · PGA · Spectral accelerations · Seismic hazard

Introduction

Iraq located on the northern portion of the Arabian Plate, as shown in Fig. 1, surrounded in the northern and eastern boundaries by the Bitlis-Zagros Fold and Thrust Belt, in which the convergent tectonic boundary between the Arabian and Eurasian plates produces a strong earthquake activity. The rest of Iraq is mainly located within the Arabian Plate, away from the major plate boundaries.

The Taurus/Bitlis and Zagros continental collision zones form the northern, northeastern and eastern boundaries of Iraq. They are the result of continued convergence between the Arabian plate and the Turkish and Iranian plateaus. The Taurus zone is diffused, but the Zagros is well defined and extends for about 1500 km in a NW-SE direction.

Figure 1 shows the northeast trending transitional motion and counterclockwise rotational motion of the plate. Most of the seismicity are occurring in the crust along the Zagros and Taurus mountain ranges and their foothills. The great majority of the earthquakes occur as a result of the continental collision between the Arabian plate and the Iranian and Turkish plateaus. Preliminary analysis of the earthquakes' spatial distribution suggests likely alignment with the faults in the region, (Ghalib and Aleqabi/JZS 2016).

Seismicity studies in Iraq can be summarized in four main studies that went a long way in *PSHA*. Three of them reached the final results in the form of contours of spectral acceleration and/or Peak Ground Acceleration, (PGA). These are, (Al-Sinawi and Al-Qasrani 2003; Mahmood et al. 1988; Onur et al. 2016):

The seismic design code of Iraq (1988) reported a seismicity study on Iraq region in which the Iraqi earthquakes data file has been collected and prepared for the period 859–1986 and the analysis of completeness indicated that the data were completed for Ms ≥ 4.8. Ten area sources were identified in the report using the reported hypocenter locations of past earthquakes listed in the Iraqi earthquake data file and with the geological and tectonics information, (Mahmood et al. 1988). The activity parameters of seismic sources such as a, b and m_{max} have been

Electronic supplementary material The online version of this article (https://doi.org/10.1007/s12517-018-3558-7) contains supplementary material, which is available to authorized users.

✉ Mustafa Shakir Farman
alishf2013@yahoo.com

[1] Civil Engineering Department, College of Engineering, University of Baghdad, Baghdad, Iraq

[2] Technical Institute of Samawa, Al-Furat Al-Awsat Technical University, Najaf, Iraq

Published online: 06 June 2018

Fig. 1 Tectonic setting of Iraq and environs (red arrows indicate plate motions in cm/year), (Onur et al. 2016)

evaluated. Also, their results have been presented in the form of contour maps of PGA using four return periods which are 50, 100, 200 and 500 years. Five attenuation relationships given by Esteva and Villaverde (1973), Donavan (1973), McGuire (1974), Fahmi and Alabbasi (1988) and Cornell et al. 1979 for the Peak ground acceleration, in terms of the magnitude and the source to site distance, were used with Poisson distribution in the PSHA to construct these maps. Also, it is found that the maps prepared by using Esteva and Villaverde (1973) attenuation relationship is more appropriate one since it correlates well with the tectonic and seismological situation of Iraq and the surrounding, (Mahmood et al. 1988).

Al-Sinawi and Al-Qasrani (2003) published a seismicity study on Iraq region that was conducted a decade before their publication. In their study, the Earthquakes data for the period 1900–1988 was used to construct contour maps of PGA for Iraq using four return periods which are 25, 50, 100 and 200 years. The seismic source modeling used by their study includes four seismic area sources and five line sources. An attenuation relationship given by Esteva and Villaverde (1973) for the Peak ground acceleration, in terms of the magnitude and the source to site distance, was used with the Poisson distribution in the *PSHA* to construct these maps. They were found that the value of PGA increases towards the east and the east-northeast.

But in these two studies, the de-clustering process not applied on the earthquakes data, that means, this data includes dependent events while Poisson distribution is used for independent events.

Also, the probability of exceedance in recent codes is 2% for 50 years life time of structures. This means, $\lambda = 4.04 \times 10^{-4}$ 1/year. Therefore, the return period $= 1/\lambda =$ 2475 years, while the larger return period that considered in the study of Al-Sinawi and Al-Qasrani (2003) is 200 years and in the seismicity study of seismic design code of Iraq (1988) is 500 years. Also, these two studies used the PGA as a ground motion intensity measure, while the recent codes and studies used the spectral acceleration at different frequencies or periods as a ground motion intensity measure.

Ameer et al. (2005) published a seismicity study on Iraq region in which the seismicity data has been prepared for the period 1905–2000 and the analysis of completeness indicated that the data were complete for $Ms \geq 4.8$ (~5.2Mw). They proposed a seismic sources model for Iraq that includes thirteen of area sources and evaluated the *a* and *b* values for each source. The maximum regional magnitude m_{max} has been evaluated to be 7.87 ± 0.86 for entire Iraq while the maximum observed magnitude was Ms = 7.2. They found that the activity parameters of the complete data for Iraq are a = 6.49 and

b = 0.89. But, their study not continued to include the whole *PSHA* process.

Onur et al. (2016) studied the seismicity of Iraq region. The earthquake catalog of their study encompasses the region between 36E-51E longitudes and 26 N–40 N latitudes, and includes about 4000 dependent events of moment magnitude 4.0, (≈2.84Ms), and larger between the years 1900 and 2009 inclusive. The analysis of completeness of seismic data indicated that they were complete to Mw ≥ 6.5. Twelve area sources were identified using the geological and tectonics information. The seismic sources parameters such as a and b were calculated for each source zone using the developed catalog while m_{max} values have been evaluated using the geometry and length of known faults within each zone. Also, contour maps of spectral acceleration at 0.2 and 1.0 s and peak ground acceleration have been constructed for a return period of 2475 years. Four attenuation relationships given by Abrahamson et al. (2014), Boore et al. (2014), Campbell and Bozorgnia (2014) and Chiou and Youngs (2014) have been used for the sources in the active shallow crustal region with the Poisson distribution in the *PSHA* to construct these maps.

Consequently, probabilistic seismic hazard analysis (PSHA) will be used to quantify the uncertainties and then to make an explicit and clear description of the distribution of future seismic intensity in terms of spectral and peak ground accelerations that may occur at a site or in other words to produce seismic hazard maps for Iraq. Firstly, the earthquake records will be collected including the recent events till the end of March 2016 and applying data processing to get the net catalog of *independent* events.

This study is divided into two stages. The first stage is collecting the earthquake records and applying data processing to get the net catalog of recorded data as explained schematically in Fig. 2. The second stage is applying the steps of the PSHA method as explained in Fig. 3.

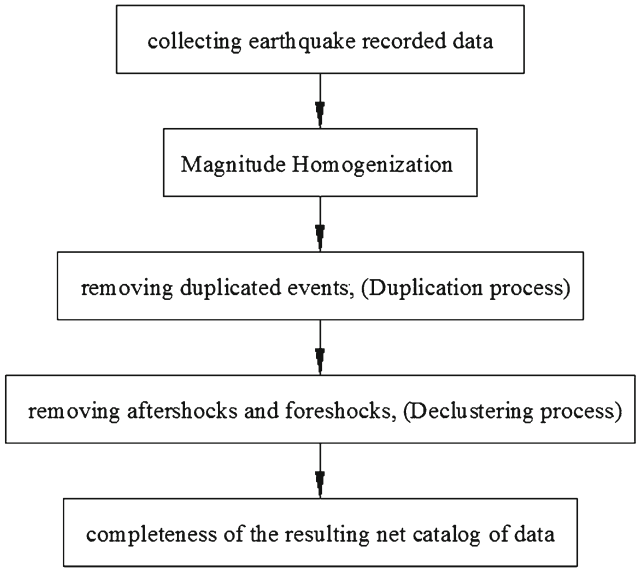

Fig. 2 Schematic sketch for earthquake data processing

Preparing and processing data

The earthquake catalog prepared for the present study of Iraq covers an area bounded by longitudes (36°.00–51°.00) E and latitudes (26°.00–40°.00) N, as that of the study of Onur et al. (2016), which are about 250 to 300 km distance to nearest boundary of Iraq.

Collecting data

The earthquake data for the study area mentioned above comprises historical data, which is before 1900, and instrumental data, which is after 1900 as shown in Fig. 4, compiled from four main sources. The first source is the Iraqi earthquakes data file from the seismic design code of Iraq (1988), which covers more than 600 earthquake events listed chronologically for the period 859–1986, which are in terms of Ms, Mb, ML. The second source is the Iranian earthquake catalog from the Iranian Institute of Earthquake Engineering and Seismology (IIEES) which covers about 8600 of events listed chronologically from 1900 up to the end of March 2016, which are in terms of Mw, Ms, M, ML. Both the Iraqi and Iranian catalogs, have their data collected from various national and regional sources such as the International Seismological Center, ISC, the United States Geological Survey earthquake data, USGS, the IIEES data, and other sources. The third source is the

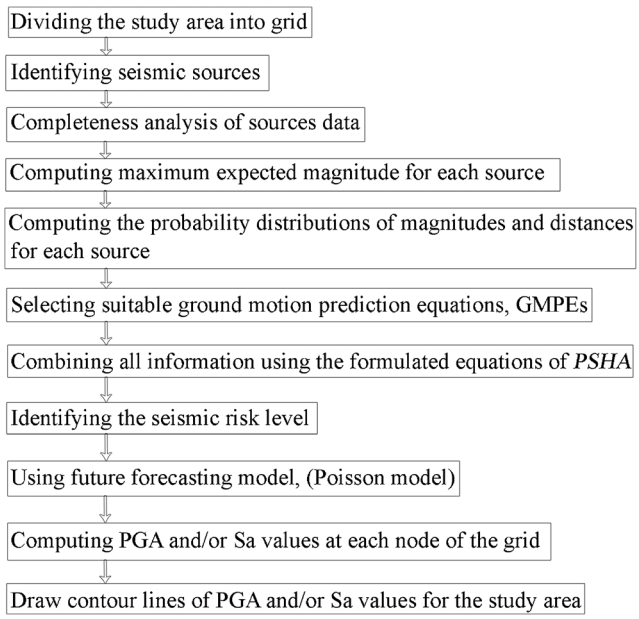

Fig. 3 Schematic sketch for PSHA method and the whole other preparing and finishing steps

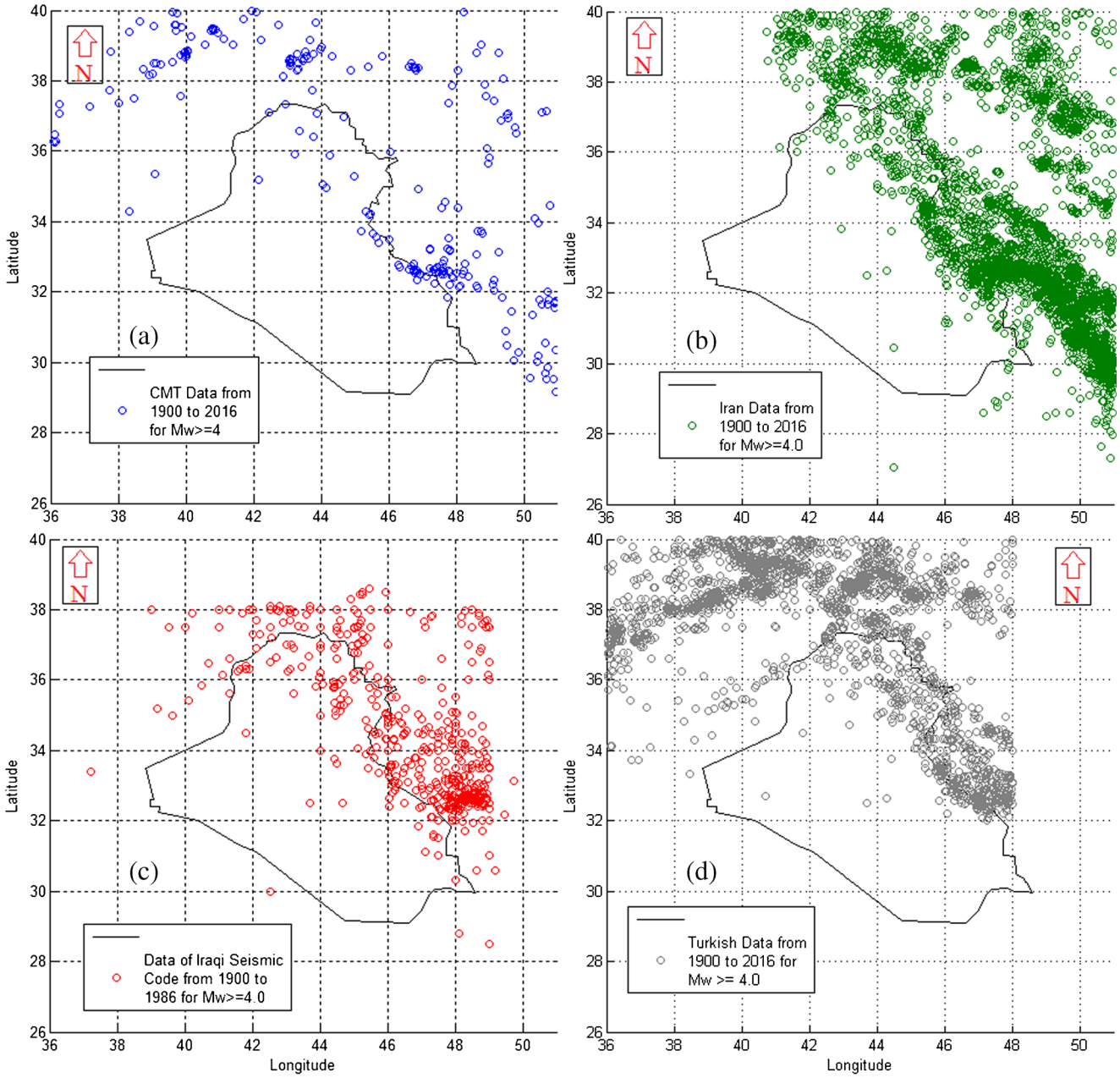

Fig. 4 The four data sources. **a** CMT data. **b** Iranian data. **c** Data of Iraqi seismic code. **d** Turkish data

global CMT catalog which covers more than 230 of events listed chronologically from 1976 up to the end of March 2016, which are in terms of Mw and Ms and Mb. The fourth source is the Turkish earthquake catalog from the Disaster and Emergency Management Authority of Turkey (AFAD) which covers about 2300 of events listed chronologically from 1900 up to the end of March 2016, which are in terms of Mw, Ms, Mb, ML.

Each of the four data sources has its special and different tabulated format, therefore; a MatLab program is built to read and deal with these different formats in order to combine and unify them in a one tabulated format of time, date, location, hypocenter depth, author and the moment magnitude scale.

Homogenization of data

Most of the contemporary GMPEs are in terms of Mw, besides that Mw is a more accurate measure of the earthquake size, especially large earthquakes, therefore; all data will be converted to Mw. Earthquake data from the above mentioned study area are used to develop relationships between the different magnitude scales. The CMT catalog provides Ms, Mw,

and Mb magnitudes for individual earthquake events, therefore; it is used to calibrate the relationships of Mw to Ms (Fig. 5) and Mw to Mb (Fig. 6). Figure 7 represents the resulted relation between Mw and ML.

As can be seen from these figures that the resulted solid-lines of fitting of Ms-Mw relations in Fig. 5 are near to that of Yazdi and Zare (2012) and that of Scordilis (2006) lines. Also, the resulted solid-line of fitting of Mb-Mw relation in Fig. 6 is near to that of Yazdi and Zare (2012) line. These relationships are formulated in Eqs. (1, 2, 3 and 4).

$$Mw = 0.632Ms + 2.1753 \quad for \quad 4 \le Ms < 5.8 \quad (1)$$

$$Mw = 0.93Ms + 0.47 \quad for \quad 5.8 \le Ms \le 7.7 \quad (2)$$

$$Mw = 0.94Mb + 0.50 \quad for \quad 4.2 \le Mb \le 6.4 \quad (3)$$

$$Mw = 0.7027Ml + 1.7247 \quad for \quad 4.2 \le Ml \le 6.2 \quad (4)$$

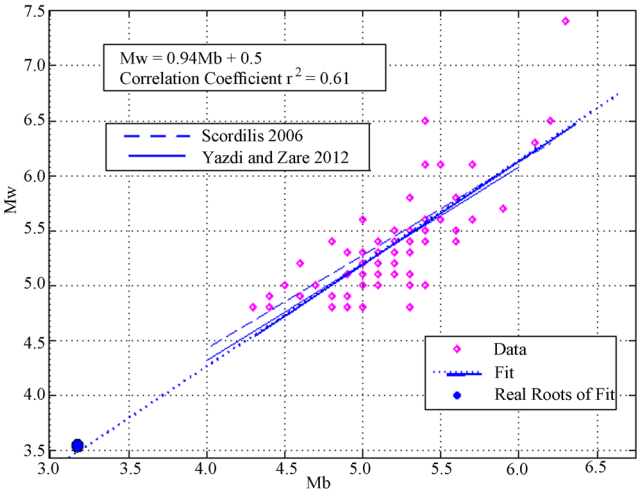

Fig. 6 Relation between *Mw* and *Mb* for the study area

Duplication

Combining the listed earthquake catalogs led to some duplicate events, which have to be removed. During this process, the following priority has been used with the sources data: Iraqi earthquake data file followed by the Iranian earthquake catalog from the Iranian Institute of Earthquake Engineering and Seismology (IIEES), and then the Turkish earthquake data catalog and finally the Global CMT catalog. Mueller et al. (1997) considered the earthquakes data are duplicated when they are from different sources and their origin times were within 1 min. While, Wheeler (2003) followed part of the Moeller procedure where he considered the data were duplicated when their origin times are within 1 day for those that before 1800, 10 h for those that before 1900, 60 min for those that before 1950 and 1 min for those that during or after 1950. He depended on the principle that the time windows are longer for older earthquakes because timekeeping may have been less accurate and reporting was often slower. He also considered similarity in location within a few tenths of degree, and similarity in magnitude within a few tenths of a magnitude unit are duplication. Nasir et al. (2013) considered the earthquakes data are duplicated if they were from different sources and with a maximum difference in longitude and/or latitude of 0.05 and/or maximum difference in time is 1 h.

The criteria of Nasir et al. (2013) will be used but with the time windows of Wheeler (2003). A MatLab program is built to read the combined data and to sort them and removing duplicated data basing on the above mentioned criteria. After combining earthquake events with magnitudes equal or greater than Mw = 4 from these four data sets, the number of events in the combined catalog were

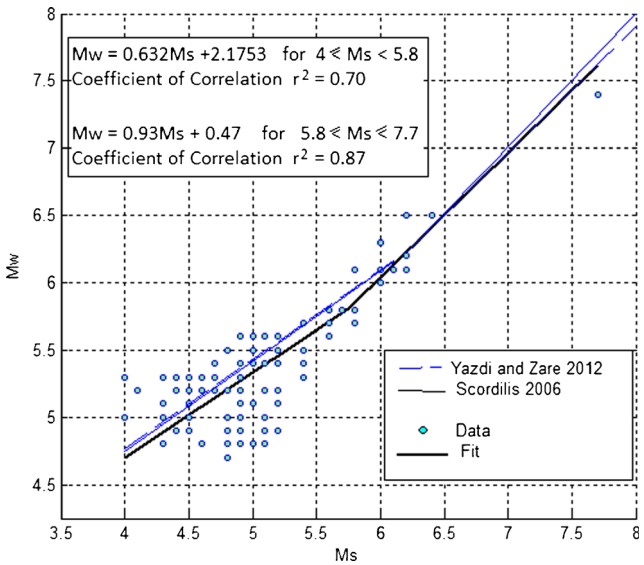

Fig. 5 Relation between *Mw* and *Ms* for the study area

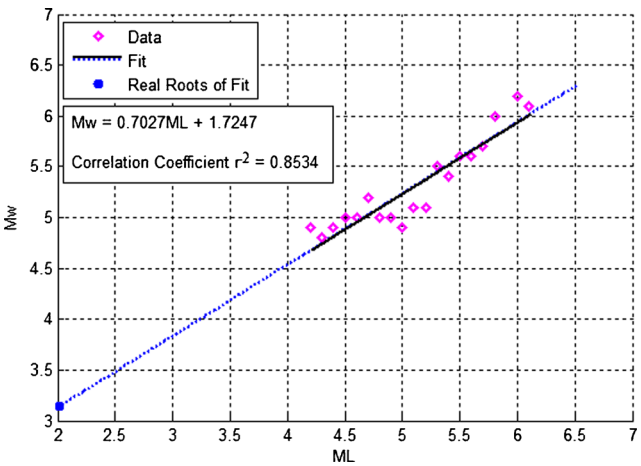

Fig. 7 Relation between *Mw* and *Ml* for the study area

7049 with 577 of duplicated events therefore, the net catalog was containing 6472 of events.

De-clustering and checking

Windowing procedures are simple ways of sorting main shocks and aftershocks basing on the general assumption that earthquakes events are Poissonian distributed. Gardner and Knopoff (1974) presented a broad windowing procedure for distance and time in terms of magnitude in a tabulated form. They applied their procedure to four catalogs and found that the fraction of aftershocks was about 2/3 of each raw catalog. The windowing algorithm given by Uhrhammer (1986) is straightforward, easy to implement and presented in two equations for distance and time, (Knopoff 2000; Uhrhammer 1986; Van Stiphout et al. 2012).

In this study, the windowing procedure based on algorithm given by Uhrhammer (1986) has been used to remove the dependent events, which are the foreshocks and aftershocks. A MatLab program is built to read the net catalog of unduplicated data and to execute the de-clustering process based on the above mentioned algorithm. This is by searching for the largest event in the net catalog. Then, computing the radius window and the time window for this event, from the above mentioned algorithm. All other events within these windows will be considered as foreshocks and aftershocks which will be removed. After that, this large event which is the main shock will be saved in another new storage and deleted from the net catalog. Finally, repeating these steps will result the catalog of independent main shocks in the new storage. The net catalog contains 6472 events, but after de-clustering, they remain only 3519 main events, which means that more than 45% of the total events have been removed by de-clustering, as shown in Fig. 8. Also, it is found that more than 90% of the remaining main earthquakes have a depth of between 0 up to 35 km, which indicates that majority of earthquakes in the study region exhibit *shallow crustal* seismic activity. These events with their information will represent the main input data file for the *PSHA* analysis.

Also, to apply chi-square test on the remaining main events to check whether they follows Poisson distribution or not, a MatLab program is built to read the data from the net catalog after de-clustering and to execute the chi-square test process. The Poisson probability distribution function is, (Freund 1994);-

$$P(k,\lambda m.t) = \frac{(\lambda m.t)^k.\, e^{-\lambda m.t}}{k!} \tag{5}$$

Where: P(k, λm.t) is the Probability of having k main events in future time period t, λm is the mean rate of occurrence.

This program started by reading the de-clustered data and then dividing the recording interval, (T years), into subintervals of 1 year, (i.e; $t = 1$), and counting the number of subintervals, (frequencies: xk), that having k = 0, 1, 2,…., N main shocks. These are the actual or the observed frequencies. The expected or Poisson frequencies, (xpk), were computed as following, (Freund 1994);

$$\lambda m = \frac{total\ number\ of\ main\ events}{total\ number\ of\ subintervals} = \frac{\sum_{k=0}^{N} k.x_k}{T} = \frac{0.x_o + 1.x_1 + \ldots}{T}$$

Then, for t = 1 year and constant mean occurrence rate λm, the Poisson probability distribution function of Eq. (5) will be rewritten as;

$$P(k) = \frac{\lambda m^k.e^{-\lambda m}}{k!} \tag{6}$$

$$xp_k = T.P(k) = T\frac{\lambda m^k.e^{-\lambda m}}{k!} \tag{7}$$

but with the condition that if xp_k reaches a value less than 5 at $k = k^*$, a value of xp with $k \geq k^*$ will be the last frequency which is equal to;-

$$xp(k \geq k^*) = T - \sum_{k=0}^{k^*-1} xp_k \tag{8}$$

and the corresponding actual or observed frequency will be;

$$x(k \geq k^*) = T - \sum_{k=0}^{k^*-1} x_k = \sum_{k=k^*}^{\infty} x_k \tag{9}$$

then, the computed chi-square, (χ^2), is;

$$\chi^2 = \sum_{k=0}^{k^*} \frac{(x_k - xp_k)^2}{xp_k} \tag{10}$$

This is compared with the values of the chi-square table, $\left(\chi^2_{v,a}\right)$, where υ = degree of freedom which is the number of terms in summation − 2 = (k^* + 1) − 2 = k^*-1 which is found to be υ = 5 for Mw ≥ 5.3, α is the level of significance which is 0.05. Then, the hypothesis of a Poissonian future forecasting distribution model will be accepted if the computed χ^2 is less than the tabulated $\chi^2_{5,0.05}$. It is found that for Mw ≥ 5.3, χ^2 = 10.8693 and $\chi^2_{5,0.05} = 11.07$ and this means all main earthquake events with Mw ≥ 5.3 in the de-clustered catalog obeys or follows a Poisson distribution, (Van Stiphout et al. 2012).

Completeness

Many methods have been proposed to evaluate the magnitude above which earthquakes data can be considered complete,

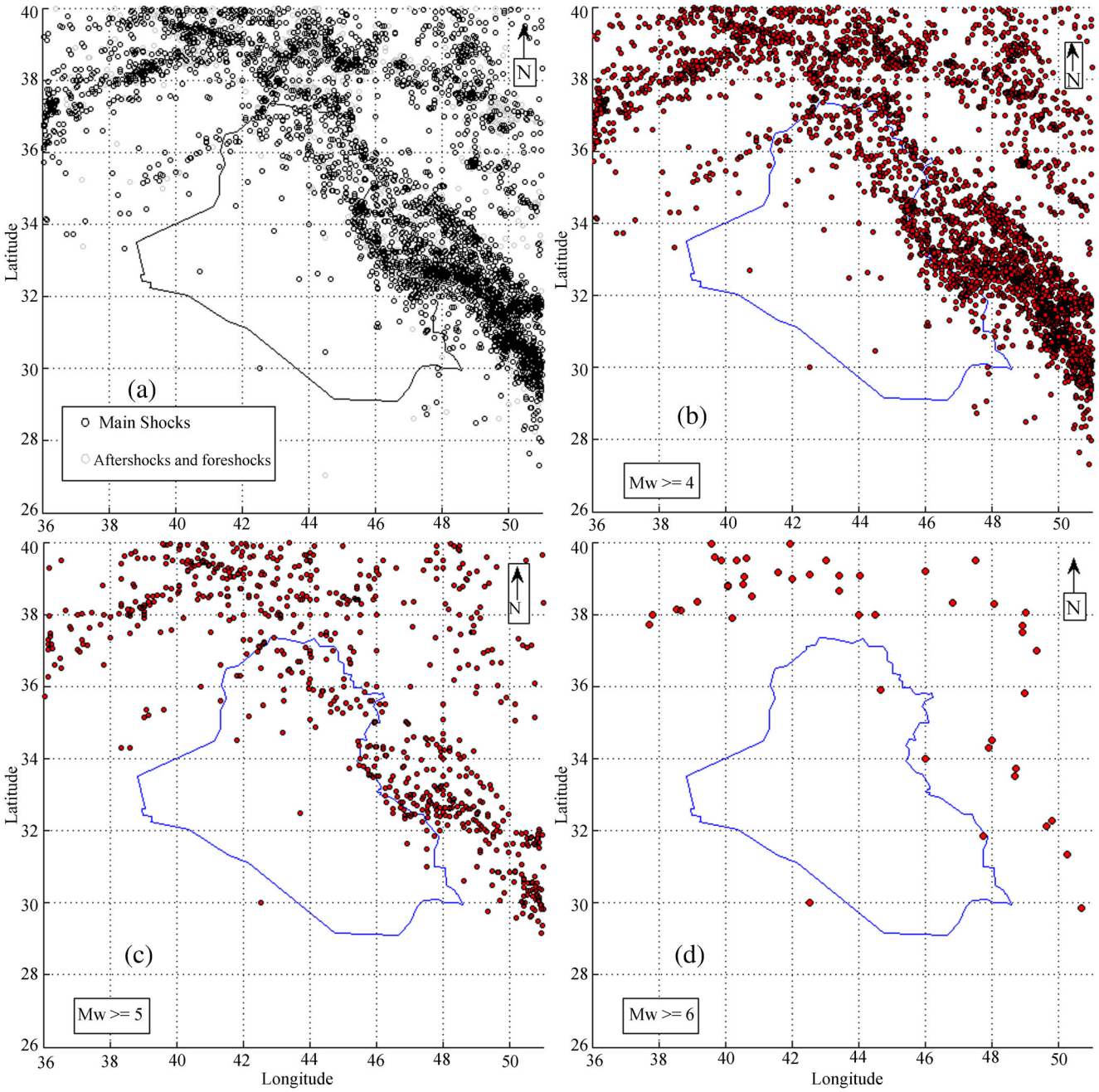

Fig. 8 The remaining main shocks for PSHA. **a** The epicentral distribution for the total 6472 shocks with Mw > = 4, gray circles are the 2953 aftershocks and foreshocks, black circles are the 3519 main shocks which are same as that in drawing (**b**), **b** main shocks with Mw > = 4, **c** main shocks with Mw > = 5, **d** main shocks with Mw > = 6

(Mc), or to specify time intervals in which a certain magnitude range can be considered to be completely reported. The statistical and graphical method proposed by Stepp (1972) is used to evaluate completeness time of the reported magnitudes.

The FMD method to estimate completeness is generally the simplest mathematical method. In this method, Mc is defined as the magnitude at and above which 90% of the data can be modeled by Gutenberg and Richter (GR) power law distribution of magnitudes, this method called Goodness of Fit, (Wiemer and Wyss 2000). The Gutenberg and Richter (1944) law is, (Baker 2008):

$$\mathrm{Log}\,\lambda_m = \mathrm{a} - \mathrm{b}.\mathrm{m} \tag{11}$$

where b and a are constants to be estimated by regression of past recorded data, λ_m is the annual rate of earthquake events with magnitudes greater than m. This relation could be linear

or bilinear on semi log paper, (Baker 2008).

To evaluate the goodness of fit, the difference between the observed FMD and a synthetic distribution must be computed. For incomplete data sets, the (GR) law cannot adequately explain the observed FMD, therefore; the difference will be high. In this method, the following steps are performed to estimate Mc, a and b:-

First, b and a values of the GR law as a function of minimum magnitude, (Mi), are estimated, based on the events with $M \geq Mi$. Using the maximum likelihood estimate, the b and a values are estimated. Next, a synthetic distribution of magnitudes with the same a, b and Mi values is computed, which represents a perfect fit to GR law. To estimate the goodness of the fit, R, the absolute difference of the number of earthquakes events in each magnitude bin between the synthetic and observed distribution is computed, then, (Wiemer and Wyss 2000):-

$$R(a, b, Mi) = 100\left(1 - \frac{\sum_{Mi}^{Mmax} |Bi - Si|}{\sum_i Bi}\right) \quad (12)$$

where Si and Bi are the predicted and observed cumulative number of earthquakes events in each magnitude bin. Dividing by the total number of observed events in order to normalize the distribution. If Mi is smaller than the right Mc, the synthetic distribution based on GR law cannot model the FMD adequately. Therefore; the goodness of fit which computed in percent of total number of earthquakes events, is poor. The goodness-of-fit R increases with increasing Mi until reaches a maximum value of R. At this Mc, the GR simple power law with the computed a and b values can explain R% of the data variability. And beyond this Mi, R may decrease gradually. But, Mc is defined as the point at which the GR simple power law can model 90% or more of the FMD. Figure 9a represents the temporal distribution of earthquakes in the harmonized de-clustered catalog which provide an indication for completeness periods.

Completeness analysis was performed using the tested de-clustered catalog for the whole area under study and for each source zone by using the goodness of fit method which was converted into a MatLab program. It is found that the data set of the de-clustered catalog are complete for $Mw \geq 5.4$ since 1900 where $a = 6.3776$ and $b = 1.1227$, Fig. 10a. As an example for seismic sources, Fig. 10b represents the result of completeness analysis for source zone 9. Also, by using the Stepp method, it is found that the completeness intervals for the de-clustered catalog are as following: $5.5 <= Mw < 6$ are complete since 1900, $5.0 <= Mw < 5.5$ since 1937, $4.5 <= Mw < 5$ since 1967, $4.0 <= Mw < 4.5$ since 1987, Fig. 11a. These results have been fitted to GR law after extrapolating the recurrences of the previous intervals along the total period and then presented in Fig. 11b where $a = 6.45$ and $b = 1.1234$, which are near to that of Goodness of fit in Fig. 10a. It is important to mention that all the programs used for processing and preparing the data have been checked manually.

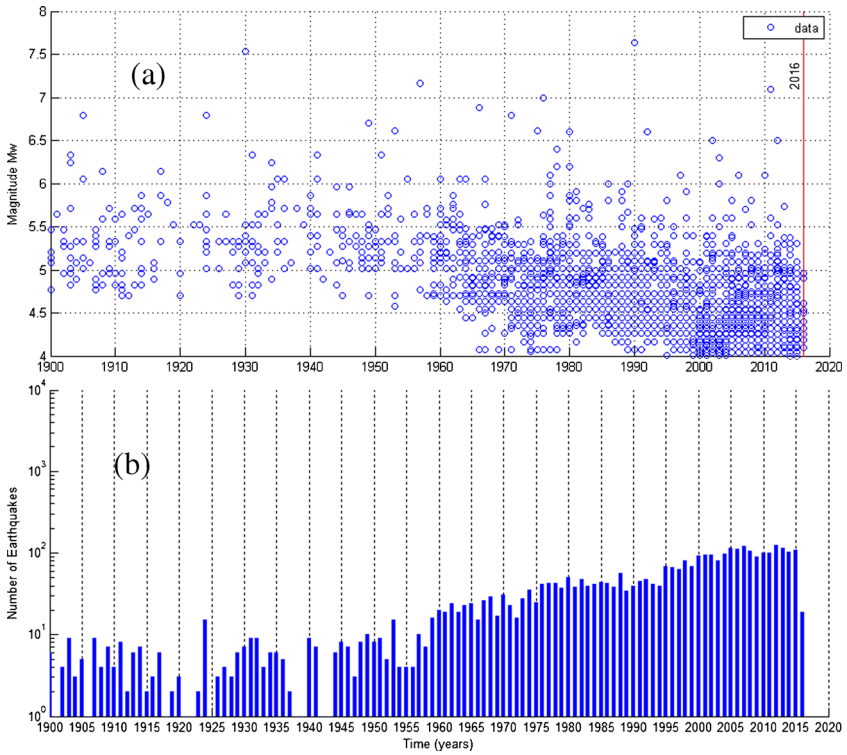

Fig. 9 **a** Temporal distribution of earthquakes in the harmonized de-clustered catalog. **b** Number of earthquakes in the harmonized de-clustered catalog by year

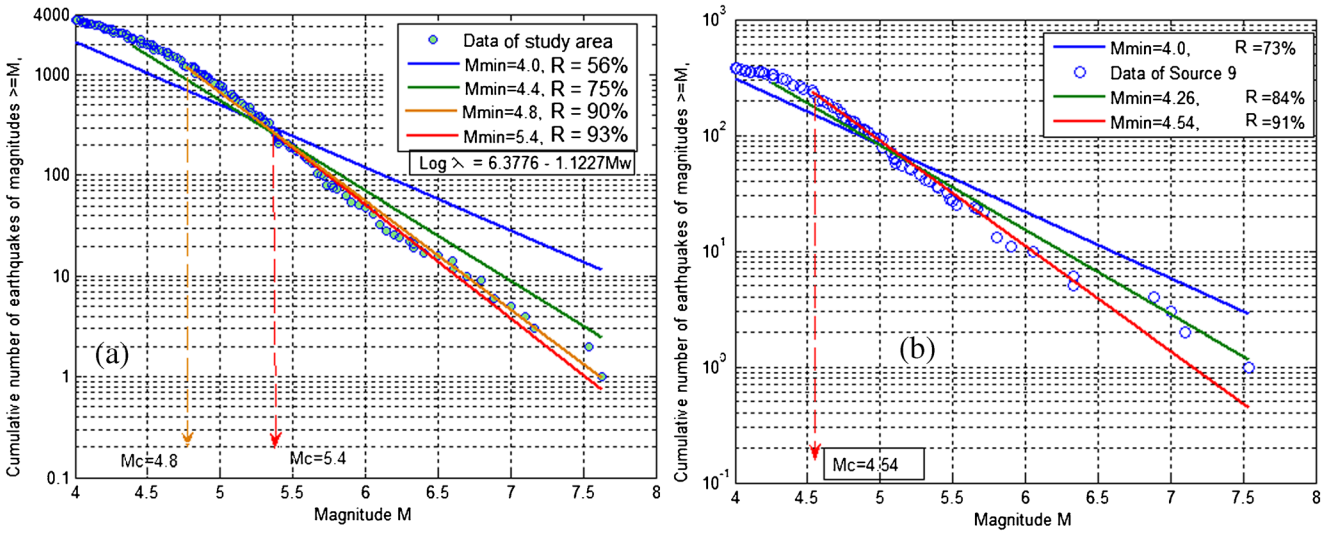

Fig. 10 Completeness analysis using Goodness of fit for: **a** the whole study area. **b** Source 9

Formulation of the *PSHA*

Formulation of the *PSHA* is mainly concerned with estimation of the expected occurrence rate, λ (*IM* > *x*), of exceeding a specified value, *x*, of the seismicity intensity measure, *IM*, that used for definition or characterization of hazard at a site. The original formulation of Cornell (1968) and Kramer (1996) will be used for this purpose. All *PSHA* information can be combined to define the occurrence rate using total probability theorem as following, (Baker 2008; Gupta 2007);-

$$\lambda(IM > x) = \sum_{i=1}^{n_{sources}} \lambda_m(Mi > m_{min}) \sum_{j=1}^{n_M} \sum_{k=1}^{n_R} P(IM > x \mid m_j, r_k) P(M_i = m_j) P(R_i = r_k) \tag{13}$$

Where:

P(IM > x | r, m) is computed from the ground motion prediction equation, (GMPE). Most of GMPEs give the ground motion intensity measure in terms of its mean logarithm, ($\widehat{Log\,IM}$). Then, using the normal distribution, (Baker 2008);-

$$P(IM > x \mid r, m) = 1 - \phi\left[\frac{Logx - \widehat{Log\,IM}}{\sigma_{LogIM}}\right] \tag{14}$$

σ_{LogIM} is the standard deviation given by the used ground motion prediction model.

$P(R_i = r_k)$ and $P(M_i = m_j)$ are the discretized probabilities of occurrences for distance and magnitude, and the summations over all considered distances and magnitudes. The conditional probabilities of exceedance from all possible distances and magnitudes are add up by the summation operations. Each conditional probability of exceedance is weighted by the probability of occurrence of the related distance and magnitude.

n_R and n_M are intervals of the discretized ranges of possible *Ri* and *Mi*, respectively, for each seismic source *i*.

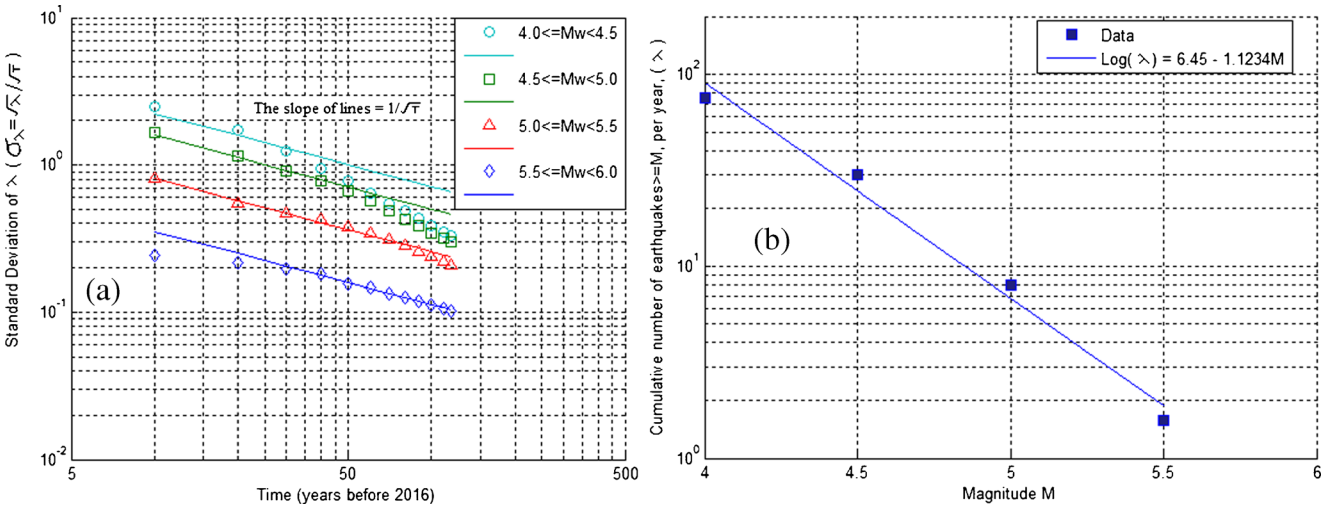

Fig. 11 Completeness analysis for the study area using Stepp method: **a** Completeness intervals. **b** Fitting to Gutenberg and Richter 1944 law

$\lambda_m(\mathrm{M}i > \mathrm{m}_{\min})$ is the rate of occurrence of earthquakes greater than the minimum magnitude, $\mathrm{m}_{\min}$, for each seismic source i. Gutenberg and Richter (1944) law in Eq. (11) will be used to represent the seismic activity for each source, therefore; the rate $\lambda_m(\mathrm{M}i > \mathrm{m}_{\min})$ is computed from Eq. (11) for each source zone.

Earthquakes with magnitudes smaller than $\mathrm{Mw} = \mathrm{m}_{\min}$ will not be considered in the computations because of their little engineering importance, (Baker 2008).

When there are more than one source, the sum of the rates of $(IM > x)$ produced from each individual source will simply represent the rate of $(IM > x)$ from all sources.

Each area seismic source will be divided into small-size elements, the epicenter of each element will be considered to lie at the geometric center point of that element. Then, the probability distribution of epicentral distances for the area seismic source can be obtained easily from the geometric centers of its elements, (Crowley et al. 2011).

These points for the geometric centers of the elements will construct a regular grid of nodes. The nodes of this grid are equally spaced in longitude and latitude. The location of each node is defined by one geographic coordinate which are (longitude, latitude), and with their units are decimal degrees. The nodes contained within the polygon of an area source represent, in a discrete way, this area source. The spacing measured in kilometers between the nodes depends on the latitude. Actually, the spacing between any two neighboring nodes near to the equator is greater than at higher latitudes. This means that the elements have their shape tends to be squeezed as moving upward or downward towards the poles, (Crowley et al. 2011).

Consequently, in order to guarantee the homogeneity of the distribution of seismicity, an easy method is adopted in which the seismicity is distributed proportionally to the element size. Particularly, for the seismic activity to be uniformly distributed, each of the epicentral locations of elements is assigned a weight in proportion with their areas, (Crowley et al. 2011; Gupta 2007; Gupta 2013), using the following relationship;-

$$P(R_i = r_k) = \frac{A_{elem,k}}{A_{src}} \tag{15}$$

where $A_{elem,\ k}$ is the area of element k, and computed by the following relationship;-

$$A_{elem,k} = 4\pi.spc^2.\left[\frac{earth-radius}{360}\right]^2 \cos(Latitude\ of\ element\ center) \tag{16}$$

where: spc is the distance in degrees between each two contiguous grid nodes adopted to discretize the seismic area source, and earth-radius is defined as the mean radius of the Earth and it is equals to 6371 km, (Crowley et al. 2011). A_{src} is the total source area and is computed as;-

$$A_{src} = \sum_{k=1}^{n_R} A_{elem,k} \tag{17}$$

where n_R is the number of elements or nodes within the area source, (Crowley et al. 2011).

Also, the element-to-site distance r_k is computed using spherical law of cosines;-

$$r_k = \left(\frac{\pi}{180}\right) radius\ of\ earth.cos^{-1}(\sin(Lat1).\sin(Lat2) + \cos(Lat1).\cos(Lat2).\cos(long2 - long1)) \tag{18}$$

Using Eq. (11), the cumulative distribution function (CDF) for M is, (Baker 2008; Gupta 2007);-

$$F_{Mi}(m) = \frac{1-10^{-\mathrm{b}(\mathrm{mi}-\mathrm{mi}_{\min})}}{1-10^{-\mathrm{b}(\mathrm{mi}_{\max}-\mathrm{mi}_{\min})}}, \qquad where; \qquad mi_{min} < mi < mi_{max} \tag{19}$$

where mi_{max} is the maximum earthquake magnitude that a given seismic source i can produce. This limited distribution of magnitudes is termed as the bounded Gutenberg-Richter recurrence law. Finally,

$$P(M_i = m_j) = F_{M_i}(m_{j+1}) - F_{M_i}(m_j) \tag{20}$$

where m_j are the discrete range of earthquake magnitudes, arranged so that $m_j < m_{j+1} = m_j + dm$.

In Eq. (20), the probabilities of all magnitudes between the values m_{j+1} and m_j are assigned to the discrete value m_j. As much as the discrete magnitudes become closely spaced, this approximate procedure will not affect numerical results. Thus, a practical *PSHA* analysis uses small magnitude spacing, (dm), equals or less than 0.1, (Baker 2008), a value of $dm = 0.1$ will be used here.

Earthquake occurrences with time

According to Poisson's assumption, the probability of observing at least one earthquake event with magnitude $M > m$ in a period of time t is computed as, (Baker 2008);

$$P(M > m) = 1 - e^{-\lambda m.t} \quad (21)$$

Equation (21) can be expressed in terms of the probability that the ground motion exceeds the test level x at least once during a specified time interval t as, (Gupta 2007);

$$P(IM > x) = 1 - e^{(-\lambda.t)} \quad (22)$$

The rate λ in Eq. (22) is the same as λ(IM > x) from Eq. (13), therefore; Eqs. (13) and (22) as will be seen later are used in conjunction.

Methodology used in applying *PSHA* steps on Iraq

The *PSHA* is conducted for Iraq taking into account the newly compiled data set. After the data has became ready, to apply the *PSHA* method, a number of subroutines have been constructed and connected together using MatLab. Each one executes one of the steps of *PSHA*, or prepare to execute the steps of *PSHA*. Also, a main program has been constructed to call these subroutines to execute the whole steps of *PSHA* method in a sequential manner according to sequence of the *PSHA* steps. This program will be tested with another work and/or program later before the end of this section.

Identifying seismic sources

There is no enough information about the dimensions and geometry of the active main faults in Iraq, therefore; the area source type will be used to represent the effective seismic sources and with a uniform seismicity rates. Hence, the twelve area sources that identified and used by Onur et al. (2016) will be used in this study because they cover all the area of Iraq and most of its surrounding regions and their events. Thus, Fig. 12 represents the spatial distribution of the used seismic hazard source model with the epicentral locations of the data of the final net catalog.

Referring to Fig. 12, most of the data are in the sources lying along the border region of Iran and Turkey, i.e. in the *active shallow crustal region*. Figure 13 illustrates the method used to identify each area source and to sort the data according to their sources, where;

(x_o, y_o),(x_f, y_f): are the lower left and upper right points of the study area, in degrees. *spc*: is the interval of the used grid in both directions, in degrees. *nc*: is the number of sources.

Then, the data will be distributed to the identified sources according to their coordinates and accordingly their

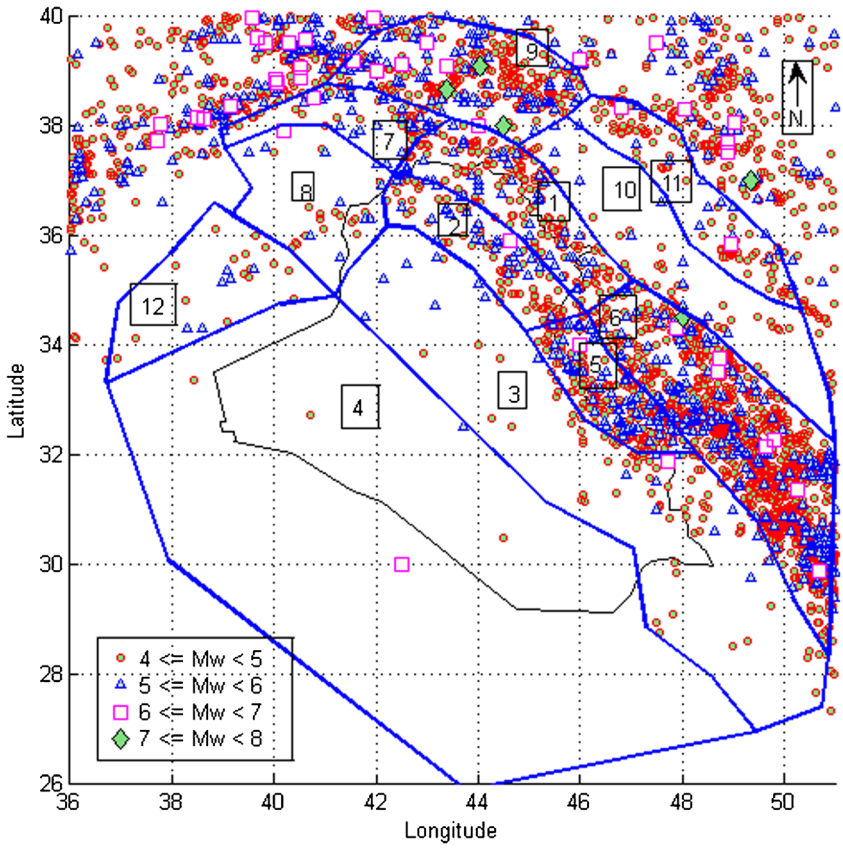

Fig. 12 The epicentral locations of earthquakes of the final net catalog

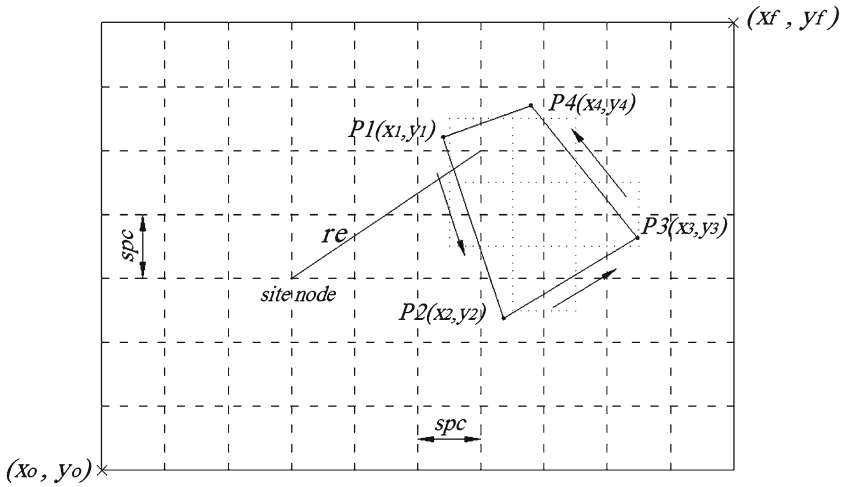

Fig. 13 Identifying input method of study area and seismic sources

boundaries. The output will be the data and the number of data for each source.

Identifying earthquake distances

After identifying each seismic source by the small elements, then, the distance from each grid node inside the source, (geometric center of each source element), to any grid node within the study area, (site), is considered as the epicentral distance, (r_e), to that site. This distance will be computed by using Eq. (18) which will be used later in the ground motion prediction equations (GMPEs). For each source, this distance is computed for each element from its center to each grid node, (site). Using *spc* equals 0.5°, the number of the grid nodes will be 899, thus, this distance will be computed 899 times for each source element of the twelve sources. Also, the area of each source element and the total area of each source will be computed using Eqs. (16, 17), respectively. This is to compute $P(R_i = r_k)$ from Eq. (15) to be used later in the *PSHA* main equation, (Eq. (13)).

Identifying earthquake magnitudes

The discrete probability distribution of magnitudes for each source will be computed using equations (19, 20). A magnitude increment $dm = 0.1$ will be used in Eq. (20). But to use Eq. (19), the maximum expected magnitude, m_{max}, need to be specified or computed for each source. The Kijko and Singh (2011) method to compute m_{max} will be used, depending on the observed m_{max} from the historical and instrumental data. But, this solution needs the values of the completeness magnitude M_c, b and the remaining data from the output of the completeness analysis of each source. Hence, the completeness analysis need to be applied firstly, using the goodness of fit, for each source, (Wiemer and Wyss 2000). Also, a minimum magnitude of Mw = 4.3 will be used for all sources. Table 1 represents the activity parameters of all sources.

Ground motion intensity

When there is no available sufficient strong motion data, generally a number of ground motion intensity models are selected, and then these models will be combined through a logic-tree approach, (Bommer et al. 2005). As mentioned by Cotton et al. (2006), the process of selecting the ground-motion models should lead to the smallest number of independent GMPEs that capture the possible ground motions in the study region. For this purpose, they proposed a criteria includes many steps. Through these steps, reasons should be found for exclusion rather than for inclusion. This criteria could be considered for rejecting equations and eliminating them from the complete list of the available candidate models.

Among the more general ground motion intensity equations developed worldwide, the European equations are built according to data sets caused by shallow crustal earthquakes that include many records from the Middle Eastern countries

Table 1 Activity parameters of sources zones, ($Mw_{min} = 4.3$ for all sources)

Source zone no.	Mc	G-R: a-value	G-R: b-value	Max. expected magnitude
1	4.7	5.3194	1.1457	7.15
2	4.4	4.3580	1.0857	7.72
3	4.0	3.0025	0.7768	7.35
4	4.7	2.1633	0.6569	7.35
5	4.8	5.3663	1.1305	7.05
6	4.6	5.8573	1.1169	7.42
7	4.9	4.9072	1.0667	7.17
8	4.9	4.9537	1.1886	5.97
9	4.6	4.9250	1.0024	7.79
10	4.4	3.3359	0.8107	7.42
11	4.3	3.0316	0.7896	7.20
12	4.3	2.7140	0.7755	5.75

such as Jordan, Turkey, Syria, Algeria, Iran and Armenia. Most of these countries are surrounding the active boundaries of Iraq, (Akkar et al. 2014; Douglas 2016). This motivates using these relations as candidate models according to Cotton et al. (2006) criteria. Also, to ensure the independence or there is no overlap or the overlap is partial in data sets from which ground-motion models were generated, candidate models based on data sets caused by shallow crustal earthquakes that contain global records will be considered, (Boore et al. 2014; Douglas 2016). The two GMPEs of Akkar et al. 2014 and Boore et al. 2014 will be used for active regions. Also, two GMPEs from NGA East project (stable regions) will be used for west stable region of Iraq, these are Pezeshk et al. (2015) and Al Noman and Cramer (2015). The uncertainties in source characterization and GMPEs are summarized in the logic tree shown in Fig. 14.

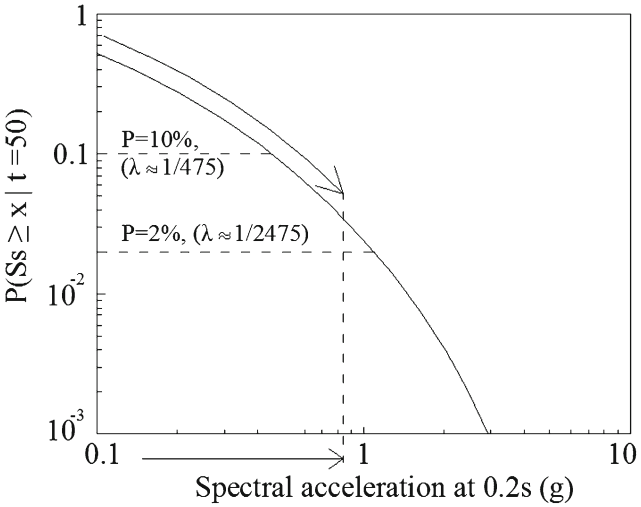

Fig. 15 An example of a hazard curve

Applying *PSHA* equations on Iraq

The probability level (2%), the soil type, and all of the ground motion parameters selected correspond to the requirements in the revision and update of the Iraqi building codes. The computations were performed for 5% damping PGA and Sa at 0.2 s and 1.0 s and for 2% probability of exceedance in an interval of 50 years, and for rock sites.

The main program will execute the two main equations of *PSHA*, Eqs. (13) and (22), and applies a method concluded from the hazard curve principle to compute the value of *IM* at each site. Referring to Fig. 15, it starts by using *IM* values starting from the lowest one and then, continuously increased by an equal increments. As the *IM* value increases, the probability of exceedance decreases until it reaches a value of 0.02 or just less than 0.02, in other word, the value of $\lambda(IM > x)$, which is the result of Eq. (13), becomes less than (1/2475). At this instant, the value of *IM* will be saved as it is the value at that site grid node, and so on for other grid nodes. Therefore; the output will be the value of the peak ground acceleration or spectral acceleration at any period with a probability of exceedance of 2% and with a life time of 50 years, (2475 years return period). This will be at each site grid node, which means the output will be a data file which contains 899 of values for each run or for each ground motion intensity measure, (acceleration), to be computed. Finally, the output values are plotted as a contour map of PGA or Sa for the study region.

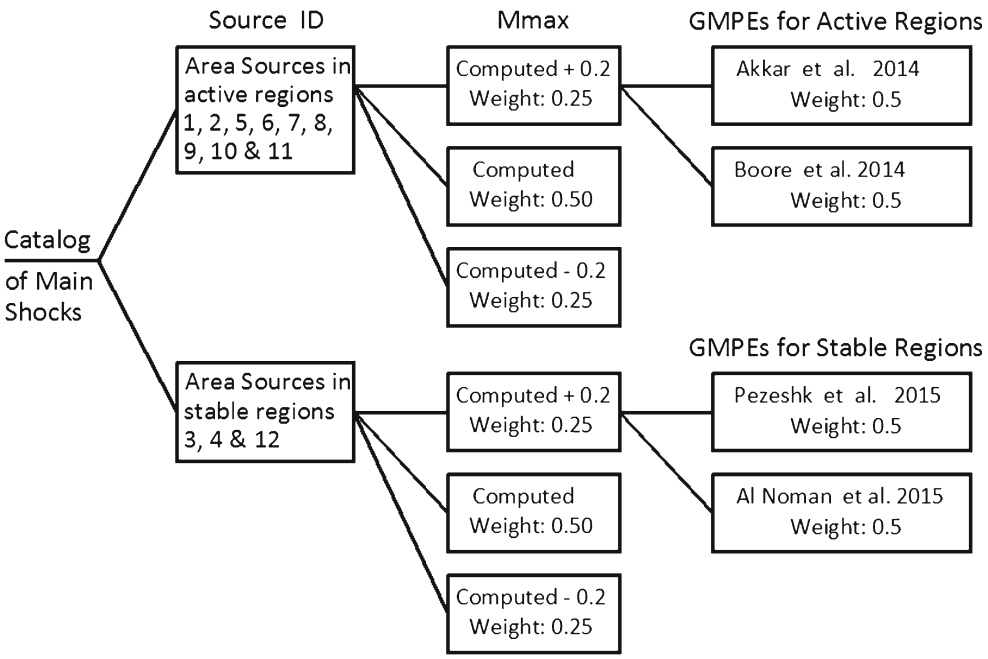

Fig. 14 Logic tree used for source and ground motion characterization

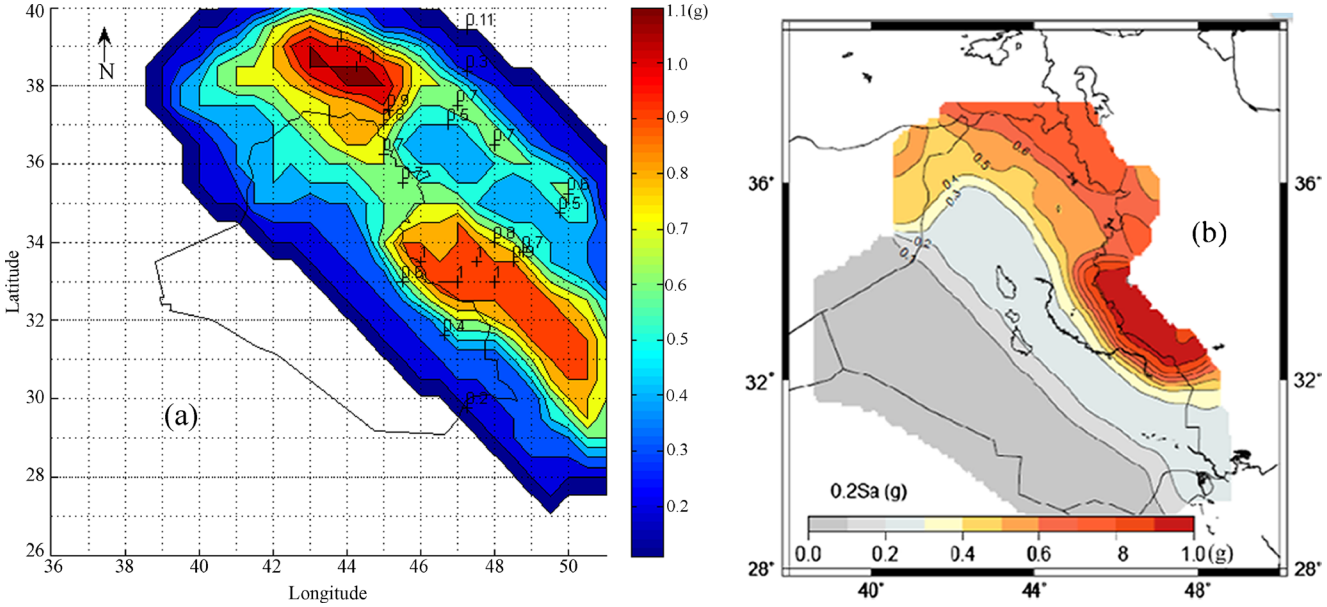

Fig. 16 Spectral accelerations at 0.2 s for a return period of 2475 years on Site Class B, in units of (g), based on activity parameters (a, b, Mmin and Mmax) from Onur et al. (2016): **a** Results of the constructed program of this study. **b** Results of Onur et al. (2016)

Checking the constructed program

In order to test the work of the constructed program with another program or another work, it is important to mention that the limits of the study area and the seismic source model adopted in this study and then in the constructed program are the same as that used by Onur et al. (2016) and they used EqHaz software. From this it can be concluded that if the same activity values, (*a, b, Mmin, Mmax*), are used, the work and results of the constructed program can be tested indirectly with the EqHaz software as compared to their results. This comparison is illustrated in Fig. 16 in terms of spectral accelerations at 0.2 s.

This comparison reveals the similarity in behavior and very close values especially in the interior and boundary of Iraq. A very small difference in values at some places due to the difference in the used GMPEs and used logic tree.

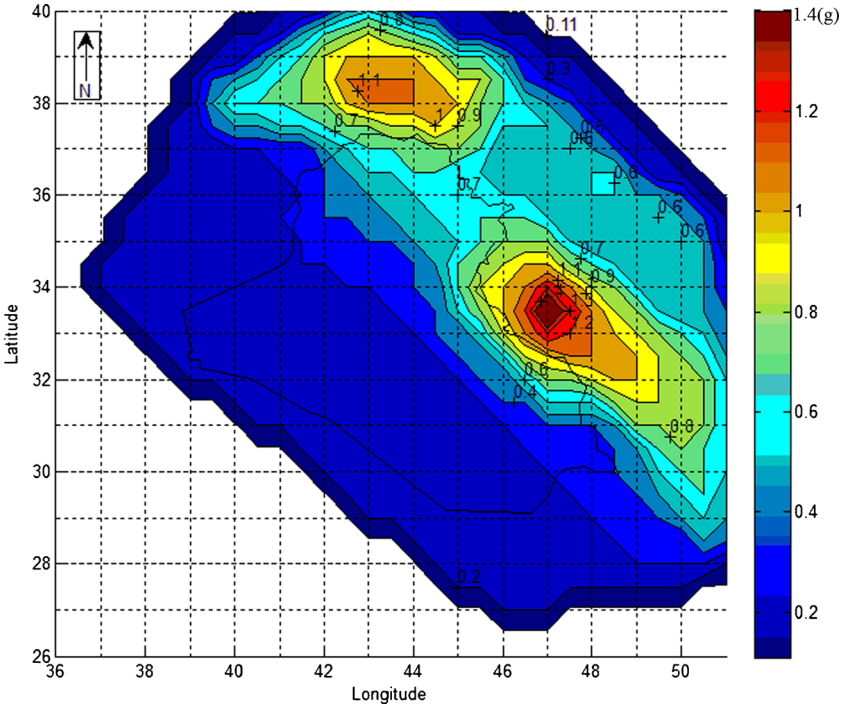

Fig. 17 Spectral accelerations at 0.2 s for a return period of 2475 years on Site Class B, in units of (g)

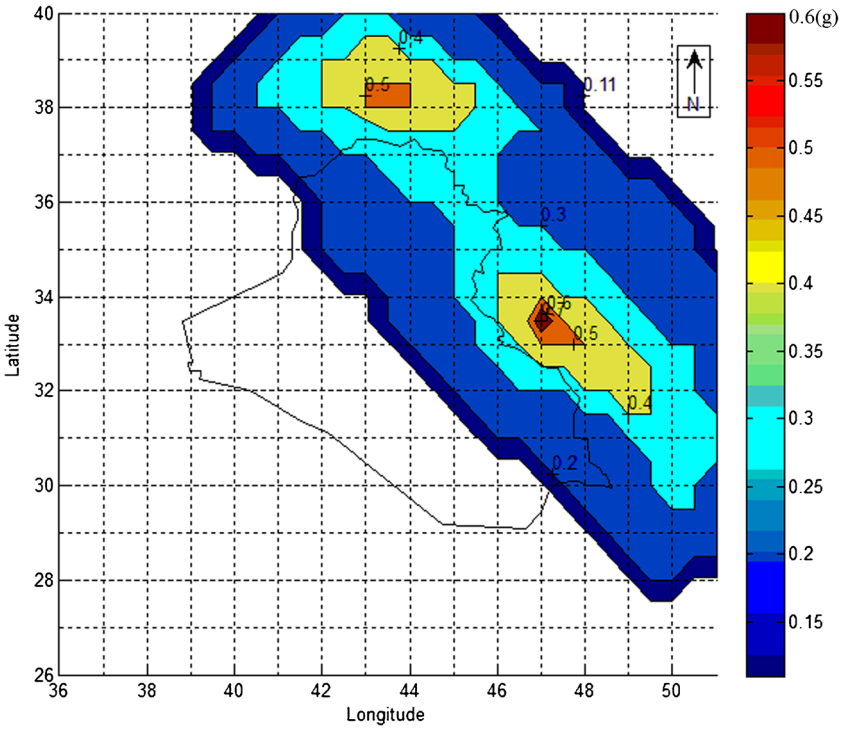

Fig. 18 Spectral accelerations at 1.0 s for a return period of 2475 years on Site Class B, in units of (g)

Results

Figures 17, 18 and 19 represent the results of this study in the form of contour maps of spectral accelerations at 0.2 and 1.0 s and PGA for a return period of 2475 years. The values increases towards the east-northeast and north as the convergent tectonic boundary between the Arabian and Eurasian plates produces a strong earthquake activity.

That is why the strong earthquakes are increased which recently struck the border areas with Iran, specifically, the 12 November 2017 (7.3Mw) earthquake, which occurred at southern part of source no. 2, as shown in Fig. 20, and it is

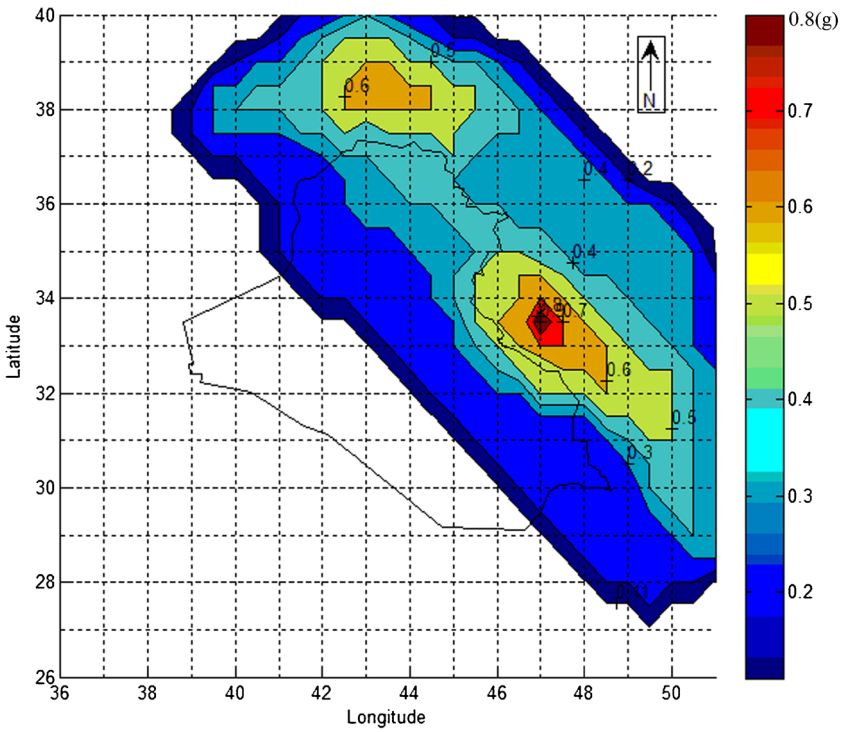

Fig. 19 The peak ground accelerations for a return period of 2475 years on Site Class B, in units of (g)

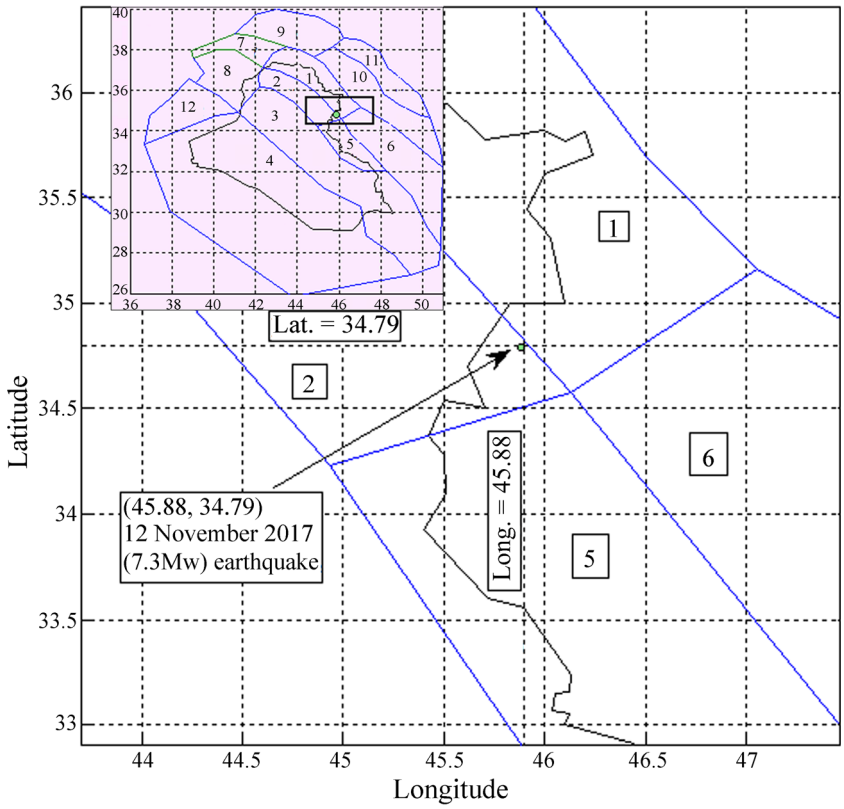

Fig. 20 The location of the 12 November 2017 (7.3Mw) earthquake

less than the expected maximum magnitude for source no. 2, Table 1. Accordingly, other stronger earthquakes are expected to occur in this region.

Also, Fig. 21 represents the design spectra for three selected main cities.

Comparison with neighbor countries

The PGA map for a probability of exceedance of 10% in a time interval of 50 years, (i.e; a return period of 475 years), has been plotted and then prepared together with similar maps of Iran and Turkey in one map, as presented in Fig. 22, for comparison purpose.

It can be seen from Fig. 22, that the PGA values, at border of Iraq with Turkey, are gradually increasing eastwards from about 100 cm/s^2 to about 200 cm/s^2 at Turkish side and from about 150 cm/s^2 to about 250 cm/s^2 at Iraqi side, indicating an agreement in behavior and a relative agreement but with a little bit more in values. It is worth mentioning here that the GMPE of Akkar et al. 2014 used in this study is also one of the GMPE's that have been used with the highest weight in constructing the Turkish hazard map.

While for eastern border of Iraq with Iran, the PGA values and behavior reveal a relatively good agreement but

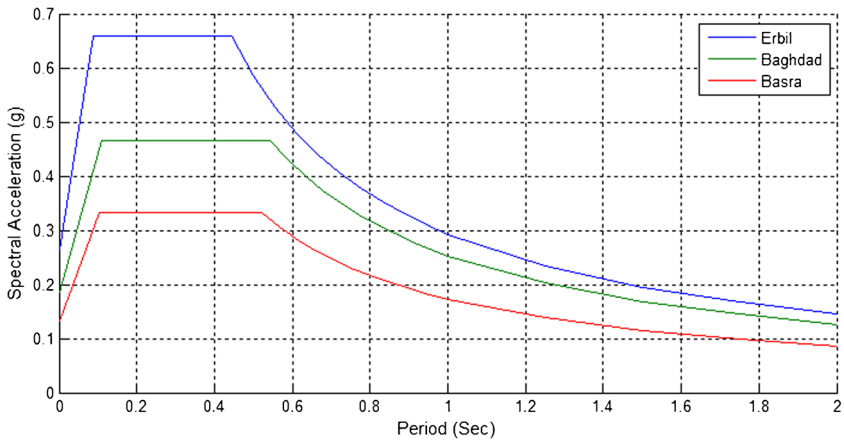

Fig. 21 Design spectra for selected cities

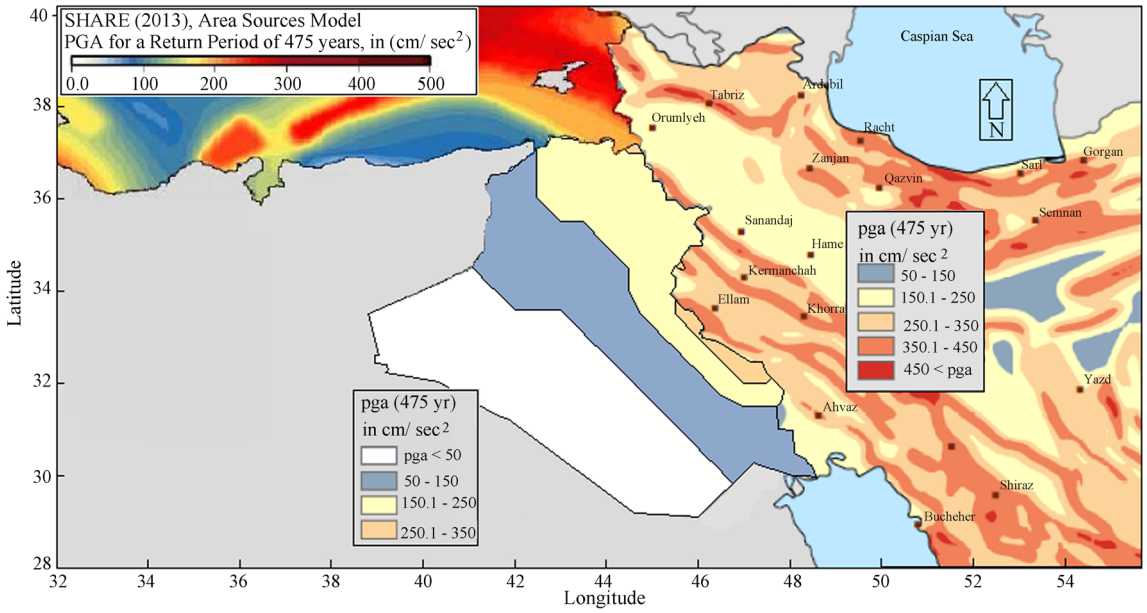

Fig. 22 The peak ground accelerations of Iraq for a return period of 475 years from this study, compared with similar maps of Iran and Turkey, (Akkar et al. 2015; Hamzehloo et al. 2012)

with a little bit less in values, just in the parts between latitudes 35.5 to 36.0 and at latitude 35, where the PGA values are clearly lesser than that of Iranian values. This is because one of the used GMPE's in this study is applied for a range of relatively small distances besides the clear difference between the seismic source models used for the region of these parts, also, all GMPE's used in Iranian work are differ than that used here.

In general, the PGA behavior is similar to that in Iran and Turkey but, the values of this study reveal a relative agreement and they are between the Turkish and Iranian values.

Conclusions

This paper presented the methodology and results of a comprehensive study executed to be as an aid to prepare the recent seismic hazard zoning maps of Iraq.

After removing duplicated data and applying de-clustering to the collected data, more than 45% of the total events have been removed. Also, it is found that more than 90% of the remaining main earthquakes have a depth of between 0 up to 35 km, which indicates that majority of earthquakes in the study region exhibit *shallow crustal* seismic activity. The remaining main earthquake events with $Mw \geq 5.3$ in the de-clustered catalog follow Poisson distribution.

Completeness analysis was performed using the tested de-clustered catalog for the whole area under study and for each source zone. It is found that the data set of the de-clustered catalog are complete for $Mw \geq 5.4$ since 1900 where the activity parameters were $a = 6.3776$ and $b = 1.1227$.

Also, by using the Stepp method, it is found that the completeness intervals for the de-clustered catalog are as following: $5.5 <= Mw < 6$ are complete since 1900, $5.0 <= Mw < 5.5$ since 1937, $4.5 <= Mw < 5$ since 1967, $4.0 <= Mw < 4.5$ since 1987. These results have been fitted to GR law after extrapolating the recurrences of the previous intervals along the total period. Then from this fitting, it is found that $a = 6.45$ and $b = 1.1234$, which are near to that of Goodness of fit.

Also, the constructed Matlab program for PSHA analysis has been checked and tested with other work and indirectly with EqHaz software, the comparison reveals good agreement in results.

The result of the PSHA method in this study was in the form of contours of PGA and spectral accelerations at 0.2 and 1.0 s for a return period of 2475 years. The values increases towards the east-northeast and north as the convergent tectonic boundary between the Arabian and Eurasian plates produces a strong earthquake activity.

For comparison purpose, the PGA map of Iraq for a return period of 475 years has also been conducted in this study. In general, the comparison of PGA with that in Turkey and Iran indicates the similarity in behavior but, the values of this study reveal a relative agreement and they are between Turkish and Iranian values. Therefore, this finding reveals the need to a teamwork between the countries in the region aims to develop a unified map of seismic hazard in this region. Especially as the seismic activity in the border areas with Iran and Turkey has recently grown strongly, specifically, the 12 November 2017 (7.3Mw) earthquake, which occurred at southern part

of source no. 2, and it is less than the expected maximum magnitude for source no. 2. Accordingly, other stronger earthquakes are expected to occur in this region.

References

Abrahamson NA, Silva WJ, Kamai R (2014) Summary of the ASK14 Ground Motion Relation for Active Crustal Regions. Earthquake Spectra 30(3):1025–1055. https://doi.org/10.1193/070913EQS198M

Akkar S, et al (2015) An overview of seismic hazard of Turkey, revision of Turkish seismic hazard map. http://scinetnathaz.net/wp-content/uploads/2015/12/Seismic_Hazard_Erdik.pdf

Akkar S, Sandikkaya MA, Bommer JJ (2014) Empirical ground-motion models for point- and extended-source crustal earthquake scenarios in Europe and the Middle East. Bull Earthq Eng 12:359–387. https://doi.org/10.1007/s10518-013-9461-4

Al Noman MN, Cramer CH (2015) Empirical ground-motion prediction equations for Eastern North America. NGA-East: median ground-motion models for the Central and Eastern North America Region. PEER Report No 2015/04, p 193–212

Al-Sinawi SA, Al-Qasrani ZO (2003) Earthquake hazards considerations for Iraq. Proc. 4rth Int. Conference of Earthquake Engineering and Seismology, Tehran, Iran. https://www.researchgate.net/publication/239528250

Ameer AS, Sharma ML, Wason HR, Alsinawi SA (2005) Probabilistic seismic hazard assessment for Iraq using complete earthquake catalogue files. Journal of Pure Appl Geophys 162:951–966

Baker JW (2008) An Introduction to Probabilistic Seismic Hazard Analysis (PSHA). Version 1.3

Bommer JJ, Scherbaum F, Bungum H, Cotton F, Sabetta F (2005) On the use of logic trees for ground-motion prediction equations in seismic hazard analysis. Bull Seismol Soc Am 95(2):377–389

Boore DM, Stewart JP, Atkinson GM (2014) NGA-West2 equations for predicting response spectral accelerations for shallow crustal earthquakes. PEER Report 2013/05, PEER Center, Headquarters, University of California, Berkeley, May 2013. http://peer.berkeley.edu/publications/peer_reports.html

Campbell KW, Bozorgnia Y (2014) NGA-West2 ground motion model for the average horizontal components of PGA, PGV, and 5% damped linear acceleration response spectra. Earthquake Spectra 30(3):1087–1115. https://doi.org/10.1193/062913EQS175M

Chiou BS-J, Youngs RR (2014) Update of the Chiou and Youngs NGA model for the average horizontal component of peak ground motion and response spectra. Earthquake Spectra 30(3):1117–1153. https://doi.org/10.1193/072813EQS219M

Cornell CA (1968) Engineering seismic risk analysis. Bull Seismol Soc Am 58(5):1583–1606

Cornell CA, Banon H, Shakal AF (1979) Seismic motion and response prediction alternatives. Earthq Eng Struct Dyn 7(4):295–315

Cotton F, Scherbaum F, Bommer JJ, Bungum H (2006) Criteria for selecting and adjusting ground- motion models for specific target regions: application to Central Europe and rock sites. J Seismol 10(2):137–156

Crowley H, Monelli D, Pagani M, Silva V, Weatherill G (2011) OpenQuake book. Version 0.1. The GEM Foundation, Pavia

Donavan NC (1973) A statistical evaluation of strong motion data including the February 9, 1971 San Fernando earthquake. Proc Fifth World Conf Earthq Eng 1:1252–1261

Douglas J (2016) Ground-motion prediction equations 1964–2016. http://www.gmpe.org.uk

Esteva L, Villaverde R (1973) Seismic risk, design spectra and structural reliability. Proc Fifth World Conf Earthq Eng 2:2586–2596

Fahmi KJ, Alabbasi JN (1988) Seismic intensity zoning and earthquake risk mapping in Iraq. Nat Hazards 1:331–340

Freund JE (1994) Mathematical statistics, 5th edn. Prentice Hall of India, New Delhi

Gardner JK, Knopoff L (1974) Is the sequence of earthquakes in Southern California, with aftershocks removed, Poissonian? Bull Seismol Soc Am 64(5):1363–1367

Ghalib & Aleqabi/JZS (2016) Seismicity, velocity structure and tectonics of the Arabian plate. J Zankoy Sulaimani, 18–1 (Part-A). Pure Appl Sci. https://doi.org/10.17656/jzs.10499

Gupta ID (2007) Probabilistic Seismic Hazard Analysis method for mapping of spectral amplitudes and other design specific quantities to estimate the earthquake effects on man-made structures. ISET Journal of Earthquake Technology, Paper No.480 44(1):127–167

Gupta ID (2013) Source-to-site distance distributions for area type of seismic sources used in PSHA applications. Nat Hazards 66:485–499

Gutenberg B, Richter CF (1944) Frequency of earthquakes in California. Bull Seismol Soc Am 34(4):185–188

Hamzehloo H, Alikhanzadeh A, Rahmani M, Ansari A (2012) Seismic hazard maps of Iran. 15WCEE, LISBOA. http://www.iitk.ac.in/nicee/wcee/article/WCEE2012_3018.pdf

Kijko A, Singh M (2011) Statistical tools for maximum possible earthquake magnitude estimation. Acta Geophys 59(4):674–700

Knopoff L (2000) The magnitude distribution of de-clustered earthquakes in Southern California. Proc Natl Acad Sci USA. 97(22):11880–11884. https://doi.org/10.1073/pnas.190241297

Kramer SL (1996) Geotechnical earthquake engineering. Prentice-Hall International series in Civil Engineering and Engineering Mechanics, Upper Saddle River, N.J

Mahmood DS, Khalifa S, Jordanovski L, Dojcinovski D (1988) Seismic hazard evaluation and seismic zoning maps of Iraq. Investigations for elaboration of preliminary seismic design code of Iraq. Building Research Center, Baghdad

McGuire RK (1974) Seismic structural response risk analysis, incorporating peak response regressions on earthquake magnitude and distance. Research Report R74–51, Massachusetts Institute of Technology, Department of Civil Engineering, Cambridge, USA

Mueller C, Hopper M, Frankel A (1997) Preparation of earthquake catalogs for the national seismic-hazard maps: contiguous 48 states. U. S. geological survey, Open- File Report 97–464, p 36. https://pubs.er.usgs.gov/publication/ofr97464

Nasir A, Lenhardt W, Hintersberger E, Decker K (2013) Assessing the completeness of historical earthquake records in Austria and surrounding Central Europe. Aust J Earth Sci 106/1:90–102 Vienna

Onur T, Gök R, Abdulnaby W, Shakir AM, Mahdi H, Numan NMS, Al-Shukri H, Chlaib HK, Ameen TH, Abd NA (2016) Probabilistic seismic hazard assessment for Iraq. LLNL-TR-691152

Pezeshk, S., Zandieh, A., Campbell, K. W., Tavakoli, B. (2015) Ground-Motion Prediction Equations for CENA Using the Hybrid Empirical Method in Conjunction with NGA-West2 Empirical Ground-Motion Models. NGA-East: Median Ground-Motion Models for the Central and Eastern North America Region. PEER Report No. 2015/04, pp. 119–147

Scordilis EM (2006) Empirical global relations converting Ms and Mb to moment magnitude. J Seismol 10:225–236

Stepp JC (1972) Analysis of completeness of the earthquake sample in the Puget sound area and its effect on statistical estimates of earthquake hazard. In: Proce International Conference on Microzonation, Seattle, USA, Vol. 2, p 897–910

Uhrhammer R (1986) Characteristics of northern and Central California seismicity. Earthq Notes 57(1):21

Van Stiphout T, Zhuang J, Marsan D (2012) Seismicity de-clustering. Community online resource for statistical seismicity analysis. http://www.corssa.org

Wheeler RL (2003) Earthquakes of the Central United States, 1795-2002 – construction of the earthquake catalog for an outreach map. U S Geological Survey, Open- File Report 03- 232, 14 P

Wiemer S, Wyss M (2000) Minimum magnitude of completeness in earthquake catalogs: examples from Alaska, the western United States, and Japan. Bull Seismol Soc Am 90:859–869

Yazdi P, Zare M (2012) Building an earthquake catalog for The Middle East. 15WCEE, LISBOA, vol. 38, p 30295